This full text paper was peer reviewed at the direction of IEEE Communications Society subject matter experts for publication in the IEEE Globecom 2010 proceedings.

Analyzing the Receiver Operating Characteristics of Novel Fiber Ring Based PON Monitoring System

Maged Abdullah Esmail and Habib Fathallah, *Member, IEEE*

Abstract— A novel ring encoder for passive optical network (PON) is proposed and analyzed in term of SNR and probability of false alarm (PFA). The encoder exploits a fiber ring and one Bragg grating to produce a multi- level periodic code. We obtain an SNR of 10 dB for 256 customers in 10ms measurement time with 20km traditional PON. For 100km long reach PON (LR-PON), we obtain an SNR of 10dB for 64 customers in very high 1.7 minutes measurement time. We also apply Neyman-Pearson testing to the receiver and we investigate how the network size affects the operational expenses of our monitoring system. We illustrate the receiver operating characteristics (ROCs) of the system showing the tradeoff between the detection and false alarm probabilities. We show that 95% detection probability (PD) for 128 traditional PON customers can be achieved with 0.006 false alarm probability (PFA) in 2ms measurement time which is 50 times smaller than PFA when averaging is not used.

***Index Terms*— FTTH, PON, optical network monitoring, signal to noise ratio, false alarm probability.**

I. INTRODUCTION

Fiber to the Home (FTTH) networks such as passive optical networks (PON) are progressively becoming reality while commercial deployments are reported worldwide [1-2]. FTTH is a network technology that has been recognized as the ultimate solution for providing various communication and multimedia services which deploys optical fiber cable directly to the home or business to deliver triple-play services, high speed internet access, digital cable television, online gaming, etc. [3]. This worldwide acceleration is largely due to both the considerable decrease in capital expenses (CAPEX) of introducing FTTH connectivity and its "future proof" nature in providing ever increasing user bandwidth requirements [4].

The passive optical network, one among several architectures that can be used in FTTH networks, is today the main choice of operators [5]. Such architecture is expected to lower the operation-and-maintenance expenses (OPEX) since there are no electronic components which are more prone to failure in the PON outside plant. There is no need for the operators to provide and monitor electrical power or maintain back-up batteries in the field.

The authors acknowledge the Prince Sultan Advanced Technologies Research Institute (PSATRI) and Saudi Telecommunication Company (STC) for their support.

Any service outage in the network can be translated into financial loss in business for the service providers [6]. When a fault occurs, technicians must be dispatched to identify, locate and fix the failure. The time, labor and truck-roll for fault identification dramatically increase the OPEX and customer dissatisfaction and complaints. Some service provides report that more than 80% of installed PON failures occurs within the first/last mile, i.e., within the distribution/drop segments of the network [7].

According to the cases reported to the Federal Communications Commission (FCC), more than one third of service disruptions are due to fiber-cable problems, and many of those disruptions have involved lifeline 911 services. Therefore, rapidly finding the cause of the disruption is critical for minimizing their effects [8]. Also one of the requirements for the next generation PON (NG-PON) is monitoring and on demand checking of the condition of optical network independently from the data traffic in the PON system. It is desirable that such monitoring and checking be available regardless of the optical network unit (ONU) is in service or even not connected [9].

There are some solutions proposed to monitor the optical access network. Some of these solutions either impose significant technical challenges or impractical due to their limited capacity [10-13]. A new technology to monitor the optical access network is to use optical codes as identifiers for the customer branches, exploited to identify the fault in the network [14]. These codes should be generated by using encoders that are passive, low power loss and cheap since the FTTH access market is cost sensitive.

In this paper, we propose a new coding scheme which is well adapted to the FTTH–PON centralized monitoring system shown in Fig. 1. Our encoder further reduces the overall cost of the monitoring system by developing simpler and lower cost optical coding devices (one ring of fiber and one simple 100% reflective Bragg grating). Note that optical rings and micro rings recently become very popular as enabling technology for the development of filters, multiplexers,

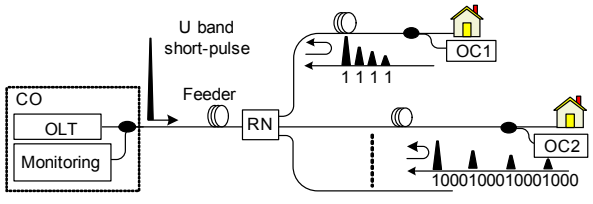

Fig. 1. Optical coding monitoring system.

978-1-4244-5638-3/10/$26.00 ©2010 IEEE

switching and channel dropping applications [15]. Compared to that of [16] where two gratings are required with two different reflectivities, this encoder replaces one of the gratings by a 2x2 coupler, hence further decreasing the encoder cost. Our results show that our new proposal supports the monitoring of a 20 km traditional PON with 256 customers and achieves SNR=10dB in 2ms measurement time.

Also we show that we can use this monitoring system for LR-PON where we found that a monitoring of 64 customers in 100km LR-PON takes 1.7 minutes measurement time to get SNR= 10dB. Moreover, we analyze our receiver in terms of probability of false alarm (PFA) and probability of detection (PD) and we use averaging to improve the performance of the receiver in detecting the fiber faults.

In section II, we introduce the monitoring system and the monitoring process. In section III, we describe the design issues of our ring based device and its operation. In section IV, we analyze the received signal and its related sources of noise. Section V shows the performance evaluation of the system and the receiver operating characteristics (ROCs) will be discussed in section VI. Finally we conclude in section VII.

II. MONITORING SYSTEM

Fig. 1 shows an optical system where a U band short pulse with peak power P_s and duration T_s is transmitted downstream from the CO in the U band (1625-1675 nm) reserved for monitoring. This pulse is split into N subpulses at the remote node (RN) using passive splitter, distributed through the DFFs to all ONUs. Each pulse close to the ONU$_i$ (i=1, 2,…., N) is encoded and reflected back to the CO by the respective optical encoders OC$_i$.

Each DDF is terminated by an encoder that generates a unique code and is located physically close to the ONU. Information on individual DDFs at the CO is discernible due to the fact that each encoder generates a unique orthogonal code.

At the CO, the received signal which is the sum of the DDF codes is decoded to determine the status of the DFF of each customer. The decoding process takes place during a specific time interval called the observation time. Without loss of generality, we assume that the receiver knows the exact observation interval for the desired customer. Indeed, the synchronization is not a part of our analysis in this paper. If the specific DDF is healthy, the monitoring code of the specific customer will be decoded and an autocorrelation peak is then identified. If a break occurs in any DDF, its code will not arrive to its specific decoder and then no autocorrelation is observed at the decoder output in the CO.

III. ENCODER DESIGN

A single incident pulse generates a code composed of w multilevel pulses that are equally spaced with a spacing p. Each customer has a Bragg grating with 100% reflectivity and a ring of fiber with length L as shown in Fig. 2.

We refer to the code as a multilevel periodic code (ML-PC).

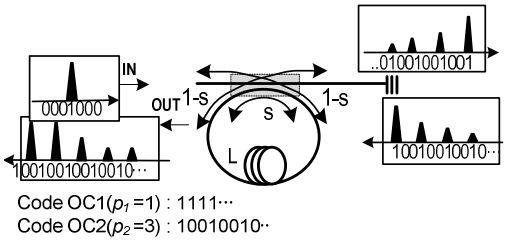

Fig. 2. Structure and operation of the proposed ring encoder.

The power coupling ratio s shown in Fig. 2 determines the amount of power that is coupled to the loop shown in Fig. 2 and that is coupled toward the Bragg grating. In extreme but unrealistic cases, when s is one, no power is coupled to the loop and the code will be only one pulse, when s is zero, all power will be coupled to the loop and no code will be generated. Realistic cases correspond to s so that $0 < s < 1$, i.e. a part of the power is coupled to the loop and a part is coupled toward the Bragg grating which is then reflected back to the ring. The part that is coupled to the loop will continue to observe other splits while traversing the coupler.

Theoretically, this splitting will continue infinitely, generating an infinite length sequence. The power level of the pulses will decrease in the sequence due to the coupling where the first pulses have the higher power level and the code can be truncated to the first w pulses.

Let ρ_j be the j^{th} pulse power level generated by the encoder and sent back to the CO. The first pulse ρ_1 corresponds to the part of the power that goes through the coupler forth and back generating a power $\rho_1=s^2$. For $j=2$ and above, the level of ρ_j can be iteratively derived as

$$\rho_j = (1-s)^2 s^{j-1} + (1-s)\rho_{j-1}, j = 2,\ldots..,w \qquad (1)$$

where w is the weight of the code. The total power for any code with weight w is expressed as

$$P_t = \sum_{j=1}^{w} \rho_j \qquad (2)$$

Fig. 3 is a plot of the coupling ratio and the total power of the code for some values of w. We notice that for $w \le 5$, the total power of the code increases as s increases. For $w > 5$, there are some values for s that cause decreasing in the total power of the code.

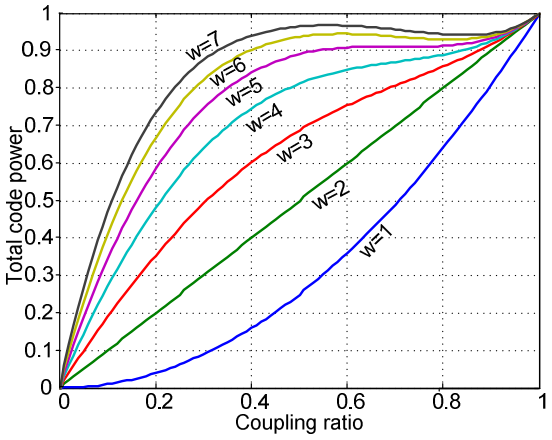

Fig. 3. Total code power as function of code weight & coupling ratio.

In the design of the codes, we seek to concentrate the reflected power in the first pulses. This avoids long codes with

greater interference between them. Also we seek to distribute this power so that all the pulses of the code have power as large as possible. Fig. 4 is a plot for the first four pulses at different values of *s* between 0.1 and 0.9 which shows the distribution of the power among these pulses. We notice visually from Fig. 3 and Fig. 4 that the interval of *s* between 0.5 and 0.6 gives good distribution (or flatness) for the power between the pulses with cumulative power that depends on the code weight *w*.

The length of the code is determined by the silent period between the pulses which is physically equal to the length of the loop *L*, shown in Fig. 2. This length is given as

$$F = pwT_s / c \tag{3}$$

where *c* is the speed of light. We need to make *F* as short as possible so that we reduce the effect of interference from the other customers. So choosing *w* is a tradeoff between the code length and the accumulative power of the code.

IV. SIGNAL AND NOISE ANALYSIS

The decoded signal for the first customer at the CO can be expressed as

$$A(t) = \sqrt{\alpha_L}\,\xi_1 e^{-\alpha_a l_1} \frac{1}{N} \sum_{j=1}^{w} \rho_j\, p(t) \tag{4}$$

where *N* is the number of customers, α_L is assumed to be the total loss due to the connectors and splices, α_a is the attenuation coefficient factor of the fiber, l_1 is the distance from the CO to the encoder of the first customer, $p(t)$ is the transmitted pulse and ξ_1 is a binary random variable that describes the health status of the DDF of the first customer with probability of fault $p(\xi_1=0)=p_0$.

In this paper we use a square law model for the detection process and we also use high gain avalanche photodiode (APD) with gain *G* and unit responsivity to compensate for the huge loss due to passive elements such as splitter/combiner. The mean of the photodetector output is proportional to the intensity of the received signal. The total output current of the photodetector is expressed as

$$\begin{aligned} i_{PD}(t) = G\left|A(t)\right|^2 + i_{BN}(t) + i_{RIN}(t) \\ + i_{SN}(t) + i_{DN}(t) + i_{TN}(t) \end{aligned} \tag{5}$$

where BN is the beat noise, RIN is the relative intensity noise,

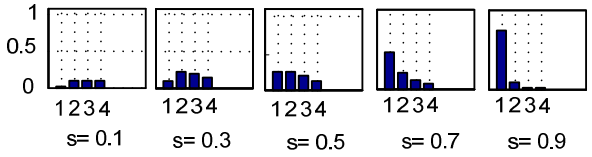

Fig. 4. Code pulses level with weight 4 and different coupling ratios.

SN is the shot noise, DN is the dark noise and TN is the thermal noise.

Using (4) and (5), the expected value of the desired signal can be expressed as

$$\overline{\sigma_s} = \frac{G\alpha_L}{N^2} k P_s e^{-2\alpha_a l_f} = \mu G P_s k \tag{6}$$

where l_f is the feeder length, $k = \sum_{j=1}^{w} \rho_j{}^2$ and $\mu = \frac{\alpha_L}{N^2} e^{-2\alpha_a l_f}$.

The relative intensity noise power, σ_{RIN}^2 is equal to the signal power multiplied by a factor β, where $\beta = \tau_c / T_s$ is ratio of the source coherence time of the optical signal to the pulse duration [17], [19]. In terms of electrical and optical bandwidths, this equation can be written as $\beta \approx B_e / B_o$ where B_e and B_o are the electrical and optical bandwidths. Using (4), the expected value of the relative intensity power can be expressed as

$$\overline{\sigma_{RIN}^2} = (1+\gamma)\beta\left[\mu G P_s k\right]^2 \tag{7}$$

where γ is the excess noise factor for the APD due to the multiplication process.

The definition of the beat noise power is similar to that of the RIN power and its expected value can be expressed as

$$\overline{\sigma_{BN}^2} = \beta m (1+\gamma)\left[\mu G P_s\right]^2 \tag{8}$$

where $m = \sum_{i=1}^{w-1} \sum_{j=i+1}^{w} \rho_i{}^2 \rho_j{}^2$. The shot noise current is modeled as a Poisson process and the average shot noise power is given as

$$\overline{\sigma_{SN}^2} = (1+\gamma) q B_e \mu G^2 P_s k \tag{9}$$

where q is the electron charge. The dark noise current is modeled as a Poisson process with an average current equal to I_{DN} and independent of all other noises as the shot noise with power $\sigma_{DN}^2 = qB_e(1+\gamma)GI_{DN}$. Thermal noise is modeled as a zero mean Gaussian process with power equal to $\sigma_{TN}^2 = N_{TN} B_e$ where N_{TN} is the power spectral density in A^2/Hz [18].

The geographical distribution of the customers is also affecting the detection process at the CO and hence the performance of the monitoring system. It is found that the uniform radial (UR) distribution, an analytically tractable distribution; gives good performance estimation and can therefore be a useful tool in characterizing performance in terms of SNR [7], [19].

V. PERFORMANCE EVALUATION

Since our monitoring system is affected by different kind of noises as discussed in section IV, we use SNR as a tool to evaluate the performance of the system.

A. Signal to noise ratio (SNR)

By definition SNR is the square of the desired signal average divided by the average of total noise power

$$SNR = \frac{\overline{\sigma_s}^2}{\overline{\sigma_n^2}} \quad (10)$$

where σ_s is the desired signal and σ_n^2 is the noise power. The noise power in (10) is the sum of power of all noises that are added to the desired signal and is expressed as

$$\sigma_n^2 = \sigma_{BN}^2 + \sigma_{RIN}^2 + \sigma_{DN}^2 + \sigma_{SN}^2 + \sigma_{SN}^2 \quad (11)$$

Consider a PON network with P_s= 4dBm, T_s =1ns and by using the parameters and values in Table I, we can plot the SNR as a function of the number of customers for a traditional PON with 20km span. We assumed a uniform distribution of customers in an area where the furthest customer's distance from the RN is small as compared to the feeder length. In Fig. 5, for 32 PON customers, our proposed monitoring system achieves 12.4 dB SNR in only one short measurement.

B. *Enhanced SNR via noise averaging*

The decoded and detected signal in the CO consists of the sum of the power coming from the desired encoder with a noise term. In an effort to reduce the noise level, we repeat the measurement *n* times and then average the noisy signals. We then reduce the variance of the noise component assuming that the repeated measurements are independent and the measurement conditions from one measurement to another do not change. This technique has been previously exploited in optical time domain reflectometer (OTDR) systems called correlated OTDR [17]. By repeating the measurements *n* times, the average noise power is $\overline{\sigma_{n-ave}}^2 = \overline{\sigma_n}^2 / n$ and the SNR can be improved by *10log n* dB [20].

In monitoring systems, the monitoring signal can be transmitted periodically during a short time interval without affecting the operation of the system which is not the case when the transmitted signal is data that needs to be transmitted continuously. This allows us to retransmit the signal *n* times and then average the detected signal to reduce the noise variance.

Using the same parameters that are used in section A with 20km traditional PON, the SNR can be improved by averaging

TABLE I
PARAMETERS USED IN THE SIMULATION

parameter	value
Code weight and coupling ratio	w= 4, s= 0.5
Fiber attunation coefficient	α_a = 0.3 dB/km
Total connector splice loss	α_L = 5 dB
Avalance photodiode	G = 100
Optical source bandwidth	B_o = 1 THz
Dark noise	I_{DN} = 160 nA
Thermal noise	N_{TN} = 10^{-26} Amp^2/Hz
Feeder length	l_f = 20 km
Fiber fault probability	P_0 = .01

where for n= 50, we can get SNR~10dB for 256 customers within 10ms measurement time as shown in Fig 5.

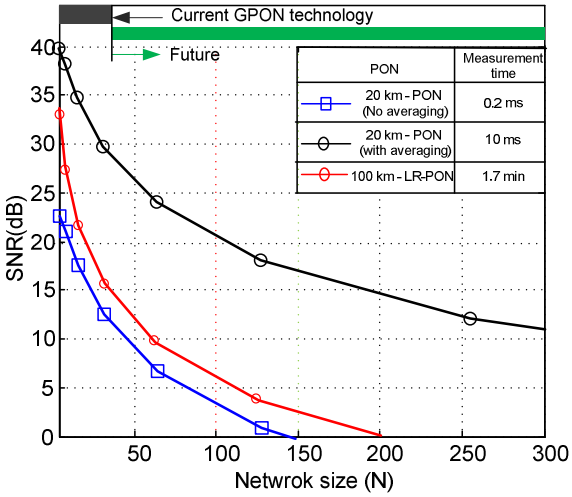

Fig. 5. SNR versus network size.

C. *Long reach PON*

Long-Reach PON (LR-PON) is a promising expansion approach for future access networks. This technology can enable broadband access for a large number of customers in the access/metro area, while decreasing CAPEX and OPEX for the network operator. The span of LR-PON technology can be increased from today's standard of 20km to 100km or higher, and thereby remotely serve high number of customers using lower number of central offices. A major challenge in LR-PON is that the propagation delay of data as well control signals between the CO and the ONUs is also increased significantly from 0.2ms RTT in traditional PON to 1ms RTT in 100km LR-PON. Also due to the long distance, the signal attenuation is high and amplifiers are needed at the local exchanges, i.e. the former central offices. Because of these challenges, the performance of LR-PON will decrease as compared to the traditional PON.

In Fig. 5 we evaluate our monitoring system as a monitoring solution for the future LR-PONs. We see that our monitoring system for example can support monitoring of 64 customers with SNR ~ 10 dB in 1.7 minutes measurement time without using amplifiers. Note that this time is very high and future research will address methods of decreasing the measurement time.

VI. FALSE ALARM AND DETECTION PROBABILITES

The presence of optical and electrical noises may cause the CO to falsely declare a broken fiber for a healthy DDF. False declaration of fiber fault results in unnecessary truck-roll and this increases the OPEX. Also the CO failure to detect a fault leads to customer dissatisfaction and complaints. Our monitoring system is similar to a multi-target radar system where both the detection P_D and false alarm P_{FA} probabilities are of great importance as in the OPEX applications [19].

We apply Neyman-Pearson testing to maximize P_D while not allowing the P_{FA} to exceed a certain value. Because the Neyman-Pearson criterion depends on specifying the P_{FA} to

yield an acceptable detection probability, we need to examine carefully how the P_D is affected by a specification of P_D versus P_{FA}. Again borrowing form radar terminology, a parametric plot of this relationship is called the *receiver operating characteristics* (ROCs) [21].

By definition P_D is the probability of correctly declaring a DDF faulty and P_{FA} is the probability of declaring a DDF faulty when it is healthy. Assuming a Gaussian distribution for the decision statistic η with mean $\overline{\sigma}_s$ and power σ_n^2, the P_D and P_{FA} are related by

$$P_D=1-Q\left(\kappa Q^{-1}(1-P_{FA})+\theta\right) \qquad (12)$$

where θ can be thought as the SNR given as $\theta \triangleq \overline{\sigma}_s(\xi_1=1)/\overline{\sigma}_n(\xi_1=1)$ and $\kappa \triangleq \overline{\sigma}_n(\xi_1=0)/\overline{\sigma}_n(\xi_1=1)$ [19].

Using P_s=4dBm, T_s=1ns and the parameters with their values in Table I, the ROCs for our monitoring system is shown in Fig. 6. For small network size, i.e. $N\leq$ 16 with no averaging, the ROCs is flat and P_D= 1 for any value of P_{FA}. As the network size increases, which means decreasing in the SNR, θ, the ROCs deteriorates.

To improve the performance of the system we use noise averaging as discussed in section V and is presented in Fig. 6. We notice that the performance is highly improved where for example, a 95% P_D for 128 customers traditional PON network can be achieved with P_{FA}=0.006 in 2ms measurement time which is 50 times smaller than PFA when averaging is not used as shown in Fig. 6 and this will highly decrease the OPEX of the network.

VII. Conclusion

We proposed and analyzed a new optical coding device that offers a promising solution for monitoring of future high-capacity PONs. We derived a mathematical model for our monitoring system and we used this model to address the importance of the network size on our monitoring system. Our optical encoding technique can support monitoring of a traditional 20km PON of 256 clients with SNR =10dB in 2ms measurement time. We also investigated the receiver operating characteristics via Neyman-Pearson hypothesis testing. Moreover, we found that 95% P_D with P_{FA}=0.006 can be achieved in 2ms measurement time for a PON with 128 customers. We extended our analysis for the case of LR-PON and we found that for 100km length, an extremely high measurement time of 1.7 minutes is required for 64 customers capacity. In future work, we will address the development of techniques to reduce the measurement time of the system.

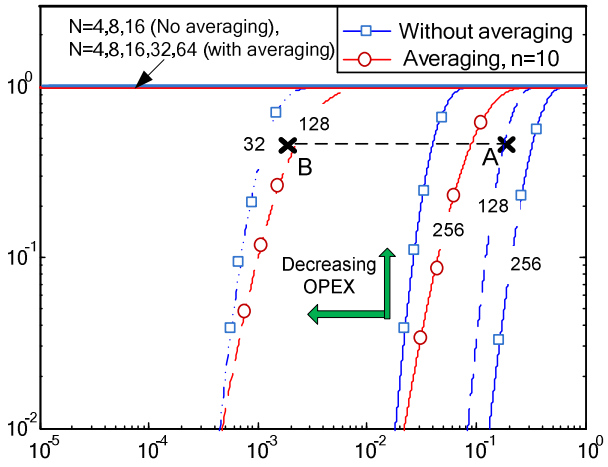

Fig. 6. Receiver operating characteristics (ROCs).

References

[1] R. Gaudino, D. Cardenas, M. Bellec, B. Charbonnier, N. Evanno, and P. Guignard, "Perspective in next-generation home networks: Toward optical solutions", *IEEE Com. Mag.*, vol. 48, issue 2, pp. 39-47, Jan. 2010.

[2] B. Batagelj, "FTTH networks deployment in Slovenia", In Proceedings of Int. Conf. on Transparent Opt. Net., pp. 1-4, Azores, July. 2009.

[3] I. Heard, "Availability and cost estimation of secured FTTH architectures", In Proc. of Int. Conf. on Opt. Net. Design and Modeling, pp. 1–6, March. 2008.

[4] K. Yuksel, V. Moeyaert, M. Wuilpart and P. Megret, "Optical layer monitoring in passive optical networks (PONs): A review", Ann. Int. Conf. on Trans. Opt. Net., vol. 1, pp. 92-98, Athens, Aug. 2008

[5] C.-H. Lee, W. Sorin, and B. Kim., "Fiber to the Home using a PON infrastructure", IEEE J. Lightw. Tech., vol. 24, pp. 4568-4583, 2006.

[6] M. Ab-Rahman, Ng Boon Chuan, M. Safnal and K. Jumari, " The overview of fiber fault localization technology in TDM-PON network", In Proc. of Int. Conf. on Elec. Design, pp. 1-8, Feb. 2009.

[7] M. Rad, H. Fathallah and L. Rusch, "Fiber Fault PON Monitoring Using Optical Coding: Effects of Customer Geographic Distribution", IEEE Trans. on Com., vol. 58, no. 4, pp. 1172-1181, April 2010.

[8] B. Masson, Ensuring the availability and reliability of dark-fiber networks. EXFO Electro-Optical Engineering Inc., pp. 1, 2005.

[9] Jun-ichi Kani, F. Bourgart, A. Cui, A. Rafel and S. Rodrigues, "Next-Generation PON—Part I: Technology Roadmap and General Requirements", IEEE Com. Mag., Nov 2009.

[10] M. Ab-Rahman, B. Ng, A. Premadi and K. Jumari, "Transmission surveillance and self-restoration against fiber fault for time division multiplexing using passive optical network", IET Com., vol. 3, issue 12, pp. 1896–1906, April 2009.

[11] N. Honda, D. Iida, H. Izumita and Y. Azuma, " In-Service Line Monitoring System in PONs Using 1650-nm Brillouin OTDR and Fibers With Individually Assigned BFSs", Journal of Lightwave Technology, vol. 27, issue: 20, pp. 4575 – 4582, August 2009.

[12] K. Yuksel, *et al*, "Centralized Optical Monitoring of Tree-structured PONs using a Raman-assisted OTDR", In Proc. of Int. Conf. on Trans. Opt. Ne., pp 175-178, Rome, Aug. 2007.

[13] C.-H. Yeh and S. Chi, "Optical fiber-fault surveillance for PONs in S-band operation window", Optics Express, vol. 13, pp. 5494-5498, July 2005.

[14] H. Fathallah, and L. Rusch, "Code division multiplexing for in-service out-of-band monitoring", J. Opt. Net., vol. 6, no. 7, pp. 819-829, July 2007.

[15] P. Yupapin and N. Pornsuwancharoen, Gudied wave optics and photonics: Micro-ring resonator design for telephone network security. Nova science publishers, 2008, ISBN 978-1-60456-838-7.

[16] H. Fathallah, M. Rad and L. Rusch, "PON Monitoring: Periodic Encoders with Low Capital and Operational Cost", IEEE Photonics technology letters, vol. 20, no. 24, December 15, 2008.

[17] D. Derickson, Fiber optic test and measurement. Prentice Hall, 1998.

[18] A. Papoulis, and S. Pillai, Probability, Random variables and stochastic processes. Forth Edition, McGraw Hill, 2002.

[19] M. Rad, H. Fathallah and L. Rusch, "Performance Analysis of Fiber Fault PON Monitoring Using Optical Coding: SNR, SNIR and False-Alarm Probability", IEEE Trans on Com., vol. 58, no. 4, April 2010.

[20] S. Antman, J. Marsden and L. Sirovich, Surveys and Tutorials in the Applied Mathematical Sciences. Springer, 2007.

[21] H. Vincent Poor, An introduction to signal detection and estimation. Springer, Second edition, 1994.